

Kinetic description of a wiggler-pumped ion-channel free-electron laser by applying the Einstein coefficient technique

A. HASANBEIGI, S. ABASIROSTAMI and H. MEHDIAN

Department of Physics and Institute for Plasma Research, Kharazmi University,
49 Dr Mofatteh Avenue, Tehran 15614, Iran
(hbeigi@tmu.ac.ir)

(Received 7 March 2013; revised 20 April 2013; accepted 30 April 2013; first published online 3 June 2013)

Abstract. A kinetic theory is used to investigate the theory of a free-electron laser with a helical wiggler and an ion channel based on the Einstein coefficient method. The laser gain in the low-gain regime is obtained for the case of a cold tenuous relativistic electron beam, where the beam plasma frequency is much less than the radiation frequency, propagating in this configuration. The resulting gain equation is analyzed numerically over a wide range of system parameters.

1. Introduction

A free-electron laser (FEL) as a continuously tunable source of intense coherent short-wavelength radiation enables the generation of laser light at ever shorter wavelengths, including extreme ultraviolet, soft X-rays and even hard rays (Seo et al. 1989; Chen and Davidson 1994; Freund and Antonsen 1996; Lambert et al. 2008). The radiation is generated by the passage of a relativistic electron beam through a periodic wiggler magnetic field generated by bifilar current windings. The purpose of the wiggler field is to provide a coupling between the electron beam and electromagnetic radiation fields, which results in a ponderomotive force along the axis of the beam. A uniform axial magnetic field is often employed to collimate the relativistic electron beam in the transverse direction. Also, the ion-channel guiding is used to focus the electrons against the self-repulsive electrostatic force generated by the beam itself. The use of the ion-channel guiding as an effective method for enhanced focusing of an intense electron beam in a single-pass FEL was offered by Takayama and Hiramatsu years ago to improve the system performance (Takayama and Hiramatsu 1988). To make an ion channel, a relativistic electron beam is injected into a pre-ionized plasma channel of uniform density. The interaction results in the formation of a positive ion core, which has arbitrary focusing and accelerating properties for electron beams, by expelling the plasma electrons along the beam. The use of the ion-channel guiding offers some merit. It is less expensive than the solenoid magnetic field (Takayama and Hiramatsu 1988). The use of the ion-channel guiding approximately solves the transverse beam breakage instability due to an intense electron beam (Jha and Kumar 1998). Another advantage of the ion-channel guiding is that the effect of the ion channel would also be to increase both the gain and efficiency of the interaction (Jha and Kumar 1996; Mahdian and Raghavi 2006;

Mahdian et al. 2008; Hasanbeigi et al. 2011; Su and Tang 2011; Sadegzadeh et al. 2012); it also permits beam currents higher than the vacuum limit. The presence of an ion channel as an electron-beam guiding device is a cost-effective alternative to the axial guide magnetic field. So, there should be higher efficiencies and lower wavelengths for the ion-channel guiding. The electron trajectories and gain in a magnetostatic helical wiggler with the ion-channel guiding have been studied by Jha and Kumar (1996). Experimental results of FEL with the ion-channel guiding have been reported by Ozaki et al. (1992) and Yu et al. (1992). The small signal gain for FEL with the ion-channel guiding has been studied in the context of quantum regime by solving the Raman–Nath equation (Mehdian et al. 2012). Mishra described the kinetic of a low gain FEL by using the Einstein coefficient method in the helical wiggler and the axial magnetic field (Mishra 2005). Also, significant progress in the quantum theory of FEL has been made by using wave kinetic (Serbeto et al. 2008).

The main purpose of this paper is to investigate the kinetic description of FEL with a helical wiggler and the ion-channel guiding by applying the Einstein coefficient technique to study the gain properties (McMullin and Davidson 1982). Although this FEL configuration has been treated previously (Mahdian and Raghavi 2006), the method employed in the present paper is completely new and can be used to study the stimulated emission at higher harmonics. The organization of the paper is as follows. In Sec. 2, the solution of the relativistic equation of motion for an electron in the presence of an ion channel and wiggler magnetic fields is presented and expanded in terms of Bessel functions. In Sec. 3, the spontaneous emission in the classical limit has been obtained and the amplitude gain per unit length has been calculated in Sec. 4 by using the Einstein coefficient method. The gain formula is quite general and can be expressed for the l th harmonic number.

Finally, the numerical studies and conclusions are given in Sec. 5.

2. General equation of motion and steady-state trajectories

Consider a relativistic electron (charge $-e$, rest mass m_e , energy $\gamma m_e c^2$) moving with velocity \mathbf{v} along the z axis of a helically polarized wiggler magnetic field with amplitude B_w and wavenumber $k_0 = 2\pi/\lambda_0$. Here, for simplicity we assume that all dynamical quantities depend only on the axial position z . In most FEL experiments, the initial beam radius is a small fraction of the wiggler period and thus this approximation is reasonable. The wiggler field may be described in one-dimensional approximation by

$$B_w = B_w(\hat{e}_x \cos k_0 z + \hat{e}_y \sin k_0 z). \tag{1}$$

The electrostatic field generated by an ion channel, with its axis coincident with the wiggler z axis, may be written as

$$\mathbf{E}_i = 2\pi e n_i(\hat{e}_x x + \hat{e}_y y), \tag{2}$$

where n_i is the density of positive ions with charge e and mass M . The relativistic equations of motion for an electron moving with velocity v in these combined fields also in the steady-state limit and laboratory frame are

$$\frac{dv_x}{dt} = -\omega_p^2 x + \Omega_w v_z \sin k_0 z, \tag{3a}$$

$$\frac{dv_y}{dt} = -\omega_p^2 y - \Omega_w v_z \cos k_0 z, \tag{3b}$$

$$\frac{dv_z}{dt} = -\Omega_w (v_x \sin k_0 z - v_y \cos k_0 z), \tag{3c}$$

where

$$\Omega_w = \frac{eB_w}{\gamma_0 mc}, \quad \omega_p^2 = \frac{2\pi n_i e^2}{\gamma_0 m} \quad \text{and} \quad \frac{d\gamma_0}{dt} = 0.$$

Once again, differentiating (3a) and (3b) with respect to time and supposing that axial velocity and energy remain constant yields

$$\frac{d^2 v_x}{dt^2} = -\omega_p^2 v_x + \Omega_w k_0 v_z^2 \cos k_0 z, \tag{4a}$$

$$\frac{d^2 v_y}{dt^2} = -\omega_p^2 v_y + \Omega_w k_0 v_z^2 \sin k_0 z. \tag{4b}$$

The solutions of these equations are

$$v_x = v_{x0} \cos \omega_p t - v_{y0} \sin \omega_p t + \frac{\Omega_w k_0 v_z^2}{\omega_p^2 - k_0^2 v_z^2} \cos k_0 z, \tag{5a}$$

$$v_y = v_{y0} \cos \omega_p t + v_{x0} \sin \omega_p t + \frac{\Omega_w k_0 v_z^2}{\omega_p^2 - k_0^2 v_z^2} \sin k_0 z. \tag{5b}$$

Substituting (5a) and (5b) into (3c) yields a differential equation for v_z which is solved as

$$v_z = v_{z0} - \frac{\Omega_w v_{x0}}{\omega_p - k_0 v_z} \cos(k_0 z - \omega_p t) - \frac{\Omega_w v_{y0}}{\omega_p - k_0 v_z} \sin(k_0 z - \omega_p t). \tag{6}$$

By integrating (6), one obtains

$$z = z_0 + v_{z0} t + \delta v_{x0} (\sin(k_0 z - \omega_p t) - \sin k_0 z) - \delta v_{y0} (\cos(k_0 z - \omega_p t) - \cos k_0 z). \tag{7}$$

Here, $\delta = \frac{\Omega_w}{(\omega_p - k_0 v_z)^2}$. It is evident from (7) that the wiggler field induces an oscillatory modulation of the axial orbit which leads to harmonic generation. In order to determine the transverse motion, (4a) and (4b) are combined to give

$$\frac{d^2 v_+}{dt^2} = -\omega_p^2 v_+ - \frac{\Omega_w}{k_0} \frac{d^2}{dt^2} e^{ik_0 z}, \tag{8}$$

where $v_+ = v_x + iv_y$. Substituting the value of z from (7) into (8) and using Bessel's identities,

$$e^{ik_0 z} = \exp i [k_0 z_0 + k_0 \delta v_{y0} \cos k_0 z_0 - k_0 \delta v_{x0} \sin k_0 z_0] \times \sum \sum J_n(k_0 \delta v_{y0}) J_m(k_0 \delta v_{x0}) \exp i [k_0 v_z t + (m+n)(k_0 z - \omega_p t)] \exp \left[-in \frac{\pi}{2} \right], \tag{9}$$

and integrating (8), one gets

$$v_+ = v_{+0} e^{i\omega_p t} + \frac{\Omega_w}{k_0} J_n(\lambda_1) J_m(\lambda_2) \times \frac{[k_0 v_z + (m+n)(k_0 v_z - \omega_p)]^2}{\omega_p^2 - [(m+n)(k_0 v_z - \omega_p) + k_0 v_z]^2} \times \exp i [k_0 z_0 + \lambda_1 \cos k_0 z_0 - \lambda_2 \sin k_0 z_0] \exp \left[-in \frac{\pi}{2} \right] \times \exp i [k_0 v_z t + (m+n)(k_0 z - \omega_p t)], \tag{10}$$

where $\lambda_1 = k_0 \delta v_{y0}$ and $\lambda_2 = k_0 \delta v_{x0}$.

3. Spontaneous emission coefficient

The spontaneous emission coefficient $\eta_w(x, p)$ is the energy radiated by an electron per unit frequency interval, solid angle and time $T = L/v_{z0}$, where the electron is accelerated in the field (Bekefi 1977). Here, L is the axial distance over which the acceleration takes place, i.e. the length of the interaction region. It is assumed that the radiation field is propagating in the Z direction with frequency ω and wavenumber k related by $\omega \approx ck$ in the tenuous beam limit. For an observation along the Z axis, the spontaneous emission coefficient in the classical

limit is given by (Bekefi 1977)

$$\eta_\omega = \frac{1}{T} \frac{d^2 I}{d\omega d\Omega} = \frac{e^2 \omega^2}{4\pi^2 c^3 T} \times \left| \int_0^T d\tau \bar{e}_z \times (\bar{e}_z \times v_+) \times e^{i(kz - \omega\tau)} \right|^2. \quad (11)$$

Here, $d^2 I/d\omega d\Omega$ is the energy radiated per unit frequency interval per unit solid angle. Substituting (9) and (10) into (11) gives

$$\begin{aligned} \eta_\omega = & \frac{e^2 \omega^2}{8\pi^2 c^3 T} \left| \int_0^\tau d\tau \left\{ v_{+0} \exp i[kz_0 \right. \right. \\ & + \lambda_3 \cos k_0 z_0 - \lambda_4 \sin k_0 z_0] j_{n'}(\lambda_3) J_{n'}(\lambda_4) \\ & \times \exp i[kv_z t + \omega_p t - \omega t + (m' + n') \times (k_0 z + \omega_p t)] \\ & \times \exp \left[-in' \frac{\pi}{2} \right] + J_{n'}(\lambda_3) J_{n'}(\lambda_4) J_n(\lambda_1) J_m(\lambda_2) \\ & \times \frac{\Omega_w}{k_0} \frac{[k_0 v_z + (m + n)(k_0 v_z - \omega_p)]^2}{\omega_p^2 - [(m + n)(k_0 v_z - \omega_p) + k_0 v_z]^2} \\ & \times \exp i \left[(k - k_0) z_0 + (\lambda_3 + \lambda_1) \cos k_0 z_0 \right. \\ & \left. - (\lambda_4 + \lambda_2) \sin k_0 z_0 \right] \exp \left[-i(n' + n) \frac{\pi}{2} \right] \\ & \times \exp i[(k v_z + k_0 v_z - \omega)t + (m' + m + n' + n) \\ & \left. \times (k_0 z - \omega_p t) \right] \left. \right\}^2, \quad (12) \end{aligned}$$

where $\lambda_3 = k\delta v_{y0}$ and $\lambda_4 = k\delta v_{x0}$. For the present purposes, the spontaneous emission coefficient η_ω for a frequency near the fundamental resonance ($m', m, n', n = 0$) obtained to form

$$\begin{aligned} \eta_\omega = & \frac{e^2 \omega^2}{8\pi^2 c^3 T} \left| \int_0^\tau d\tau \left\{ v_{+0} \right. \right. \\ & \times \exp i \left[kz_0 + \lambda_3 \cos k_0 z_0 - \lambda_4 \sin k_0 z_0 \right] J_0(\lambda_3) J_0(\lambda_4) \\ & \times \exp i \left[(k v_z + \omega_p - \omega)t \right] + \frac{\Omega_w}{k_0} \frac{k_0^2 v_z^2}{\omega_p^2 - k_0^2 v_z^2} \\ & \times \exp i \left[(k + k_0) z_0 + (\lambda_3 + \lambda_1) \cos k_0 z_0 \right. \\ & \left. - (\lambda_4 + \lambda_2) \sin k_0 z_0 \right] J_0(\lambda_3) J_0(\lambda_4) J_0(\lambda_1) \times J_0(\lambda_2) \\ & \left. \times \exp i \left[(k v_z + k_0 v_z - \omega)t \right] \right\}^2. \quad (13) \end{aligned}$$

For simplicity, (13) is now considered when the system is close to the beam resonance $(k + k_0)v_z - \omega \cong 0$. Therefore,

$$\begin{aligned} \eta_\omega = & \frac{e^2 \omega^2 T}{8\pi^2 c^3} \left\{ v_\perp^2 J_0^2(\lambda_3) J_0^2(\lambda_4) \frac{\sin^2 [(k v_z + \omega_p - \omega) \frac{T}{2}]}{\left((k v_z + \omega_p - \omega) \frac{T}{2} \right)^2} \right. \\ & + \left(\frac{\Omega_w v_z^2}{\omega_p^2 - k_0^2 v_z^2} \right)^2 J_0^2(\lambda_3) J_0^2(\lambda_4) J_0^2(\lambda_1) J_0^2(\lambda_2) \\ & \left. \times \frac{\sin^2 [(k v_z + k_0 v_z - \omega) \frac{T}{2}]}{\left((k v_z + k_0 v_z - \omega) \frac{T}{2} \right)^2} \right\}. \quad (14) \end{aligned}$$

4. Amplitude gain in the tenuous beam limit

The amplitude gain per unit length Γ determined from the classical limit of the Einstein coefficient method is given by ($\Gamma > 0$ for amplification) (Jacson 1975; Sprangle and Smith 1980)

$$\begin{aligned} \Gamma = & \frac{4\pi^3 c}{\omega^2} F \int_0^{2\pi} d\varphi \int_{-\infty}^{\infty} dp_z \int_0^{\infty} dp_\perp \bar{n}_w \frac{\gamma m}{p_\perp} \\ & \times \left[\left(\frac{\omega}{k} - v_z \right) \frac{\partial f_j^0}{\partial p_\perp} + v_\perp \frac{\partial f_j^0}{\partial p_z} \right], \quad (15) \end{aligned}$$

where F is the filling factor; $\omega = kc$ has been assumed, $v_z = p_z/\gamma m$ and $v_\perp = p_\perp/\gamma m$ are the axial and transverse velocities that are related to γ_0 as $\gamma_0 = (1 - v_z^2/c^2 - v_\perp^2/c^2)^{-1/2}$.

$$f_j^0 = \frac{N_b}{2\pi p_\perp} \delta(p_\perp - \gamma_0 m v_{\perp 0}) \delta(p_z - \gamma_0 m v_{z0}), \quad (16)$$

where $f_j^0(p_\perp^2, p_z)$ is an equilibrium distribution function, $N_b = \int d^3 p f_j^0 = \text{constant}$ is the beam density.

Substituting (14) and (16) into (15) and integrating by parts with respect to p_z and p_\perp gives the gain per unit length which is in the form

$$\begin{aligned} \Gamma = & \frac{\omega_b^2 \Gamma F}{8\gamma_0 c^2} \left\{ J_0^2(\lambda_3) J_0^2(\lambda_4) \frac{\sin^2 \psi}{\psi^2} 2 \left(\frac{c}{v_z} - 1 \right) \right. \\ & - \frac{1}{v_z^2} \left(v_\perp^2 J_0^2(\lambda_4) J_0^2(\lambda_4) \frac{\sin^2 \psi}{\psi^2} \left(\frac{k_0 \Omega_w v_z^2}{\omega_p^2 - k_0^2 v_z^2} \right)^2 \right. \\ & \left. \times J_0^2(\lambda_3) J_0^2(\lambda_4) J_0^2(\lambda_1) J_0^2(\lambda_2) \frac{\sin^2 \theta}{\theta^2} \right) \\ & + \frac{1}{v_z} \left(v_{\perp 0}^2 \times \frac{\sin^2 \psi}{\psi^2} + \left(\frac{k_0 \Omega_w v_z^2}{\omega_p^2 - k_0^2 v_z^2} \right)^2 \right. \\ & \left. \times J_0^2(\lambda_1) J_0^2(\lambda_1) \frac{\sin^2 \theta}{\theta^2} \right) \times (2J_0(\lambda_3))' J_0(\lambda_3) J_0^2(\lambda_4) \\ & \left. + 2(J_0(\lambda_4))' \times J_0(\lambda_4) J_0^2(\lambda_3) \right\} \end{aligned}$$

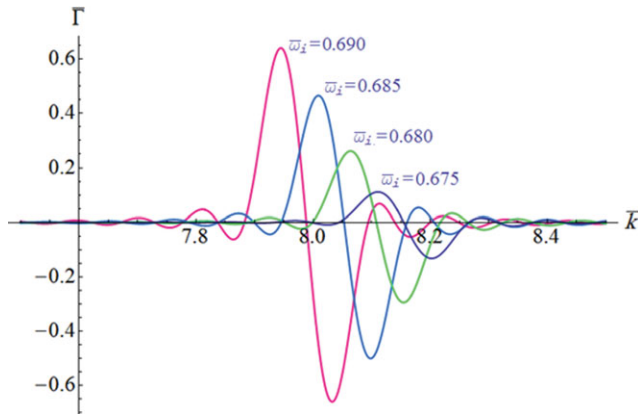


Figure 1. (Colour online) Graph of the normalized gain as a function of the normalized wavenumber for several values of the ion-channel frequency. The chosen parameters are $\gamma = 3$, $\bar{\Omega}_w = 0.1$ and $\bar{\omega}_b = 0.07$.

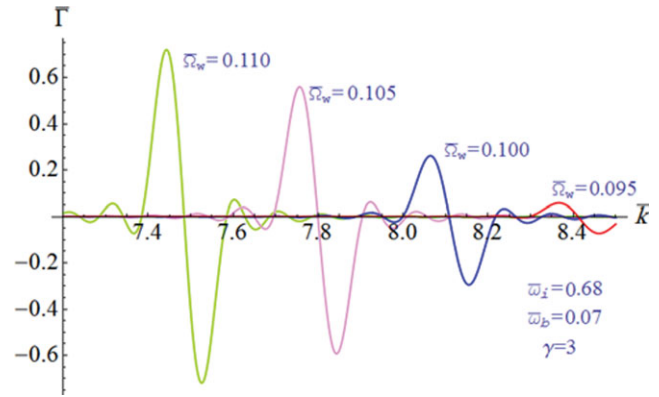


Figure 2. (Colour online) Plot of the normalized gain as a function of the normalized wavenumber for several values of the wiggler frequency. The chosen parameters are $\gamma = 3$, $\bar{\omega}_i = 0.68$ and $\bar{\omega}_b = 0.07$.

$$\begin{aligned}
 & + \frac{1}{v_z} \left(\left(\frac{k_0 \Omega_w v_z^2}{\omega_p^2 - k_0^2 v_z^2} \right)^2 J_0^2(\lambda_3) \times J_0^2(\lambda_4) \frac{\sin^2 \theta}{\theta^2} \right) \\
 & \times (2(J_0(\lambda_1))' J_0(\lambda_1) + 2(J_0(\lambda_2))' J_0(\lambda_2) J_0^2(\lambda_1)) \\
 & + \frac{1}{v_z} J_0^2(\lambda_3) J_0^2(\lambda_4) \times J_0^2(\lambda_2) \frac{\sin^2 \theta}{\theta^2} \left(\left(\frac{k_0 \Omega_w v_z^2}{\omega_p^2 - k_0^2 v_z^2} \right)^2 \right)' \\
 & + \frac{v_{\perp 0}^2}{v_z^2} \times J_0^2(\lambda_3) J_0^2(\lambda_4) \frac{L}{2v_z} \left(\omega \left(1 - \frac{v_z}{c} \right) - \omega_p \right) \\
 & \times \frac{\partial}{\partial \psi} \left(\frac{\sin^2 \psi}{\psi^2} \right) + \frac{1}{v_z^2} \left(\frac{k_0 \Omega_w v_z^2}{\omega_p^2 - k_0^2 v_z^2} \right)^2 \\
 & \times J_0^2(\lambda_3) J_0^2(\lambda_4) \times J_0^2(\lambda_1) J_0^2(\lambda_2) \frac{L}{2v_z} \\
 & \times \left(\omega \left(1 - \frac{v_z}{c} \right) \right) \frac{\partial}{\partial \theta} \left(\frac{\sin^2 \theta}{\theta^2} \right) \Bigg\}, \tag{17}
 \end{aligned}$$

where $\psi = (kv_z + \omega_p - \omega) \frac{T}{2}$, $\theta = (kv_z + k_0 v_z - \omega) \frac{T}{2}$ and $\omega_b^2 = \frac{4\pi N_b e^2}{m}$ is the non-relativistic electron frequency.

The terms proportional to L in (17) can be neglected in comparison with other terms. Therefore,

$$\begin{aligned}
 \Gamma & = \frac{\omega_b^2 L^2 \omega F}{16\gamma_0 c^2} \left\{ \frac{v_{\perp 0}^2}{v_z^2} J_0^2(\lambda_3) J_0^2(\lambda_4) \frac{\partial}{\partial \psi} \left(\frac{\sin^2 \psi}{\psi^2} \right) \right. \\
 & + \left(\frac{k_0 \Omega_w v_z}{\omega_p^2 - k_0^2 v_z^2} \right)^2 J_0^2(\lambda_3) J_0^2(\lambda_4) J_0^2(\lambda_1) J_0^2(\lambda_2) \\
 & \left. \times \frac{\partial}{\partial \theta} \left(\frac{\sin^2 \theta}{\theta^2} \right) \right\}. \tag{18}
 \end{aligned}$$

5. Results

In this section, numerical results obtained from the amplitude gain equation (18) have been presented. Shown in

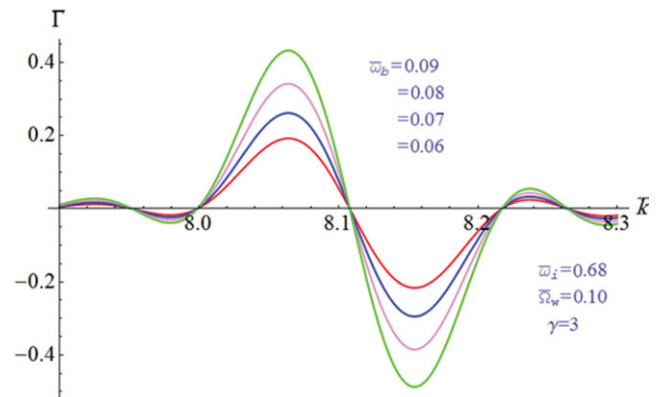


Figure 3. (Colour online) Plot of the normalized gain as a function of the normalized wavenumber for several values of the beam frequency, $\bar{\omega}_b$. The chosen parameters are $\gamma = 3$, $\bar{\omega}_i = 0.68$ and $\bar{\Omega}_w = 0.1$.

Fig. 1 are plots of the normalized gain, $\bar{\Gamma} = \Gamma/k_0$, versus the normalized wavenumber, \bar{k} , for values of $\bar{\omega}_i$ ranging from 0.675 to 0.690. The system parameters in this figure correspond to $\bar{\Omega}_w = 0.05$, $F = 0.75$, $\gamma_0 = 3$, and $\bar{\omega}_b = 0.07$. For increasing values of $\bar{\omega}_i$ corresponding to the resonance approach, it is found that there is a concomitant increase in both the maximum normalized gain and its corresponding wavelength $\lambda = 2\pi/\bar{k}$. Therefore, the gain enhancement is obtained due to the ion channel. It should be noted, however, that such enhancements in the gain correspond to increases in transverse velocity and decreases in the axial velocity of electrons due to the presence of an ion channel. The effect of the wiggler magnetic field on the gain is shown in Fig. 2, where the normalized gain is plotted as a function of the normalized wavenumber, \bar{k} , for several values of $\bar{\Omega}_w$ ranging from 0.095 to 0.11. Here, $\bar{\omega}_i = 0.68$ and the system parameters are otherwise identical to Fig. 1. As evident from this figure, the maximum gain increases with increasing the normalized wiggler frequency $\bar{\Omega}_w$. On the contrary, the wavenumber corresponding to the maximum gain decreases as the value of $\bar{\Omega}_w$ is increased. Shown in Fig. 3 are plots of $\bar{\Gamma}$ versus the normalized

wavenumber for several values of the normalized beam frequency, $\bar{\omega}_b$, ranging from 0.06 to 0.09. Here, the values of the ion channel and the wiggler frequency correspond to 0.68 and 0.1, respectively. It is seen that as the normalized beam frequency is increased to 0.09, the maximum gain increases significantly and its corresponding wavenumber remains unchanged. Therefore, the peak gain of FEL exhibits a sensitive dependence on the beam frequency. Numerical calculation shows that for a specified value of beam frequency, the gain is reduced substantially, at least at shorter wavelengths.

In summary, the kinetic model for the gain of FEL with a helical wiggler and an ion-channel guiding is explained by using the Einstein coefficient method in order to explore the dependence of the gain on the different system parameters. The steady-state electron trajectories and the gain formula for the case of a cold, mono-energetic and tenuous relativistic electron beam in the combined wiggler and ion-channel field have been investigated for various system parameters. The important conclusion for the present analysis is that for specified energy γmc^2 and the normalized beam frequency, $\bar{\omega}_b$, the maximum of the normalized gain and its corresponding wavelength increase as the normalized wiggler frequency or the ion-channel frequency is increased. On the contrary, for increasing beam frequency the maximum gain increases and its corresponding wavenumber remains unchanged.

References

- Bekefi, G. 1977 *Radiation Processes in Plasma*. New York: Wiley.
- Chen, C. and Davidson, R. C. 1994 *Phys. Rev. A* **43**, 5541.
- Freund, H. P. and Antonsen, J. M. Jr. 1996 *Principles of Free-Electron Lasers*. London: Chapman and Hall.
- Hasanbeigi, A., Mahdian, H. and Jafari, S. 2011 *Chin. Phys. B* **20**, 094103.
- Jacson, J. D. 1975 *Classical Electrodynamics*. New York: Wiley.
- Jha, P. and Kumar, P. 1996 *IEEE Trans. Plasma Sci.* **24**, 1359.
- Jha, P. and Kumar, P. 1998 *Phys. Rev. E* **57**, 2256.
- Lambert, G., Hara, T., Garzella, D., Tanikawa, T., Labat, M., Carre, B., Kitamura, H., Shintake, T., Bougeard, M., Inoue, S., Tanaka, Y., Salieres, P., Merdji, H., Chubar, O., Gobert, O., Tahara K. and Couprie, M.-E. 2008 *Nat. Phys.* **4**, 296.
- Mahdian, H., Hasanbeigi, A. and Jafari, S. 2008 *Phys. Plasma* **15**, 123101.
- Mahdian, H. and Raghavi, A. 2006 *Plasma Phys. Control. Fusion* **48**, 991.
- McMullin, W. A. and Davidson, R. C. 1982 *Phys. Rev. A* **25**, 3130.
- Mehdian, H., Alimohamadi, M. and Hasanbeigi, A. 2012 *J. Plasma Phys.* **78**, 537.
- Mishra, P. K. 2005 *Laser Phys.* **15**, 679.
- Ozaki, T. et al. 1992 *Nucl. Instrum. Methods Phys. Res. A* **318**, 101.
- Sadegzadeh, S., Hasanbeigi, A., Mehdian, H. and Alimohamadi, M. 2012 *Phys. Plasma* **19**, 023108.
- Seo, Y., Tripathi, V. K. and Liu, C. S. 1989 *Phys. Fluids B* **1**, 221.
- Serbeto, A., Mendonça, J. T., Tsui, K. H. and Bonifacio, R. 2008 *Phys. Plasmas* **15**, 013110.
- Sprangle, P. and Smith, R. A. 1980 *Phys. Rev. A* **21**, 293.
- Su, D. and Tang, C. J. 2011 *Phys. Plasmas* **18**, 023104.
- Takayama, K. and Hiramatsu, S. 1988 *Phys. Rev. A* **37**, 173.
- Yu, L. H. et al. 1992 *Nucl. Instrum. Methods Phys. Res. A* **318**, 721.